Molecules and Cells

miRNA-103a-3p Promotes Human Gastric Cancer Cell Proliferation by Targeting and Suppressing ATF7 *in vitro*

Xiaoyi Hu[1,2], Jiyu Miao[3], Min Zhang[4], Xiaofei Wang[3], Zhenzhen Wang[3], Jia Han[3], Dongdong Tong[3], and Chen Huang[1,3,*]

[1]Key Laboratory of Shaanxi Province for Craniofacial Precision Medicine Research, College of Stomatology, Xi'an Jiaotong University, Xi'an, Shaanxi, China, [2]Department of Oral Maxillofacial Surgery, Stomatological Hospital, College of Stomatology, Xi'an Jiaotong University, Xi'an, Shaanxi, China, [3]Key Laboratory of Environment and Genes Related to Diseases, College of Medicine, Xi'an Jiaotong University, Xi'an, Shaanxi, China, [4]College of Life Science, Yanan University, Yan'an, Shaanxi, China.
*Correspondence: hchen@mail.xjtu.edu.cn
http://dx.doi.org/10.14348/molcells.2018.2078
www.molcells.org

Studies have revealed that miR-103a-3p contributes to tumor growth in several human cancers, and high miR-103a-3p expression is associated with poor prognosis in advanced gastric cancer (GC) patients. Moreover, bioinformatics analysis has shown that miR-103a-3p is upregulated in The Cancer Genome Atlas (TCGA) stomach cancer cohort. These results suggest that miR-103a-3p may function as an oncogene in GC. The present study aimed to investigate the role of miR-103a-3p in human GC. miR-103a-3p expression levels were increased in 33 clinical GC specimens compared with adjacent nontumor stomach tissues. Gain- and loss-of-function studies were performed to identify the correlation between miR-103a-3p and tumorigenesis in human GC. Inhibiting miR-103a-3p suppressed GC cell proliferation and blocked the S-G2/M transition in MKN-45/SGC-7901 cells, whereas miR-103a-3p overexpression improved GC cell proliferation and promoted the S-G2/M transition *in vitro*. Bioinformatics and dual-luciferase reporter assays confirmed that ATF7 is a direct target of miR-103a-3p. Analysis of the TCGA stomach cancer cohort further revealed that miR-103a-3p expression was inversely correlated with ATF7 expression. Notably, silencing ATF7 showed similar cellular and molecular effects as miR-103a-3p overexpression, namely, increased GC cell proliferation, improved CDK2 expression and decreased P27 expression. ATF7 overexpression eliminated the effects of miR-103a-3p expression. These findings indicate that miR-103a-3p promotes the proliferation of GC cell by targeting and suppressing ATF7 *in vitro*.

Keywords: ATF7, gastric cancer, miRNA-103a-3p, proliferation

INTRODUCTION

Human gastric cancer (GC) is currently the fourth most common cancer globally and remains the most prevalent cancer in Eastern Asia (Bray et al., 2013; Strong et al., 2015). Treatment for GC includes surgery, chemotherapy or a combination of therapies. Although new strategies have been proposed to improve patient survival rates, the median survival time for advanced GC patients remains approximately 12 months (Bang et al., 2010; Koizumi et al., 2008; 2014; Tanabe et al., 2010). Thus, new treatment approaches are needed (Shen et al., 2013). In the last decades, numerous researches focused on gene expression regulatory networks in GC with expectations of improving diagnosis, therapy and prevention.

Received 15 May, 2017; revised 28 February, 2018; accepted 15 March, 2018; published online 10 May, 2018

eISSN: 0219-1032

MicroRNAs (miRNAs) are an abundant class of small non-coding RNA molecules that serve as gene regulators by base pairing and silencing mRNAs through either mRNA degradation or preventing mRNA translation. Different miRNAs can function as tumor suppressors or oncogenes in cancer cells, and the dysregulation of certain miRNAs may contribute to human cancer (Garofalo and Croce, 2011). An individual miRNA could potentially alter complex cellular processes such as cell growth, cell cycle, apoptosis and invasion. Aberrant levels of miRNAs, such as miR-16, miR-21, miR-20a, miR-372 and miR-181a, have been identified in GC and many other tumors (Cho et al., 2009; Lin et al., 2012; Shin et al., 2011; Wu et al., 2013). Recent studies have shown that miR-103a-3p is upregulated in GC, breast cancer and colorectal cancer and is thus considered an oncogene (Arabpour et al., 2016; Chen et al., 2012; Guo et al., 2015a; Hong et al., 2014; Kim et al., 2013; Nonaka et al., 2015; Rotkrua et al., 2013; Wang et al., 2012; Xia et al., 2016; Zheng et al., 2016). Based on these findings, miR-103a-3p may represent a potential diagnostic biomarker and therapeutic target in cancer. However, the regulatory mechanism remains unclear.

Activating transcription factor 7 (ATF7), a member of basic leucine zipper proteins family, is located on chromosome 12q13.13. ATF7 is phosphorylated by p38 at Thr-51 and Thr-53, leading to its transcriptional activation (Gozdecka and Breitwieser, 2012). ATF7 activities reportedly suppress tumorigenesis in mouse lymphoma models (Walczynski et al., 2014). Immunohistochemistry results in 72 post-operation colorectal cancer tissue specimens have revealed a inverse correlation between ATF7 expression and pathological stage as well as a positive correlation between ATF7 expression and 5-year overall survival or 5-year progression-free survival (Guo et al., 2015b). However, the mechanisms of ATF7 on cell proliferation in GC remain to be elucidated.

In the present study, higher miR-103a-3p levels were frequently detected in GC tissues, consistent with The Cancer Genome Atlas (TCGA) stomach cancer cohort analysis. These results indicated that miR-103a-3p may act as a tumor

Table 1. Background data among 33 patients with gastric cancer

Case	Sex	Age(y)	Size(cm)	Histologic grade	TNM stage
1	Male	55	3	Moderate	IIIc
2	Male	59	3	Moderate	I a
3	Female	61	8	Poor	IV
4	Male	69	7	Poor	IIIb
5	Male	68	8	Poor	IIIc
6	Female	67	5	Poor	IIIc
7	Male	64	5	Moderate	II b
8	Male	46	5	Poor	IIIa
9	Male	42	5	Poor	IIIc
10	Male	60	4	Poor	IIIc
11	Male	58	6	Poor	IIIb
12	Male	71	10	Poor	IV
13	Male	65	5	Poor	IIIb
14	Male	55	9	Poor	IIIc
15	Male	72	5	Moderate	IIIa
16	Female	58	11	Poor	IIIc
17	Male	78	2	Poor	I b
18	Male	66	5	Poor	IIIc
19	Male	66	2.5	Moderate	I a
20	Female	48	5	Moderate	IIIc
21	Male	50	5.5	Moderate	IIIc
22	Male	68	2	Poor	IIIc
23	Male	70	7	Poor	IIIb
24	Female	74	5	Moderate	IIIb
25	Female	55	6	Poor	IIIc
26	Male	66	5	Poor	IIIc
27	Male	48	4	Moderate	IIIb
28	Male	63	9	Moderate	IIIc
29	Male	71	6	Poor	IIIc
30	Male	59	6	Poor	IIb
31	Male	43	9	Poor	IIIb
32	Male	62	7	Poor	IIIc
33	Male	56	4	Poor	IIIb

promoter in cancer progression. To understand the underlying mechanism, additional experiments were performed *in vitro*. Overexpressing miR-103a-3p significantly improved the proliferation of gastric cancer cell lines MKN-45 and SGC-7901, while inhibiting miR-103a-3p had the opposite effect. Bioinformatics analysis and dual-luciferase reporter assays indicated that ATF7 is a novel target of miR-103a-3p. Overexpressing ATF7 suppressed MKN-45 and SGC-7901 cell growth and eliminated the effect of miR-103a-3p on GC cells, whereas ATF7 silencing via RNAi facilitated GC cell growth. Together, these results suggested that miR-103a-3p promotes cell proliferation in GC cell by targeting and suppressing ATF7. Thus, miR-103a-3p/ATF7 axis may be a promising molecular target for GC therapy.

MATERIALS AND METHODS

Cell lines and tissue specimens

Human GC cell lines, MKN-45 and SGC-7901, were obtained from the Key Laboratory of Environment and Genes Related to Diseases at Xi'an Jiaotong University (China). Cells were maintained in 1640 medium (GE, USA) supplemented with 10% FBS. A total of 33 paired gastric cancer and adjacent nontumor gastric tissues were collected from patients undergoing GC resection at the general surgery department of the First Affiliated Hospital, Xi'an Jiaotong University (China). The relevant characteristics of the studied subjects are shown in Table 1. No local or systemic treatment was administered prior to surgery. Both tumor and nontumor tissues were validated by pathologic examination. The study was approved by the Institute Research Ethics Committee at Cancer, Xi'an Jiaotong University, and all patients provided written informed consent. Tissue samples were immediately frozen in liquid nitrogen until subsequent RNA extraction.

RNA extraction and quantitative real-time PCR

Total RNA was extracted from prepared tissue or cell samples using TRIzol reagent (Invitrogen Life Technologies, USA), and cDNA was synthesized according to the manufacturer's instructions (Takara, Japan). Quantitative real-time PCR (qRT-PCR) was performed using RealStar SYBR Green qPCR Power Mixture (GenStar, China) on an FTC-3000TM System (Funglyn Biotech Inc., Toronto, Canada) according to the manufacturer's instructions. Relative gene expression (miR-103a-3p, U6, ATF7, β-actin, CDK2 and P27) was calculated using the $2^{-\Delta\Delta Ct}$ method (Livak and Schmittgen, 2001). The primers used are listed in Table 2.

Construction of expression plasmids

pEGFP-C1 was used to construct the ATF7 re-expression vector. ATF7 cDNA was chemically synthesized and cloned into pEGFP-C1 between the *Bgl*II and *Eco*RI sites. Vector was

Table 2. Primers

Name	Sequence (5'-3')
β-actin-F	CCAACCGCGAGAAGATGA
β-actin-R	CCAGAGGCGTACAGGGATAG
U6-RT	CGCTTCACGAATTTGCGTGTCAT
U6-F	GCTTCGGCAGCACATATACTAAAAT
U6-R	CGCTTCACGAATTTGCGTGTCAT
miR-103a-RT	GTCGTATCCAGTGCGTGTCGTGGAGTCGGCAATTGCACTGGATACGACTCATAGC
miR-103a-3p-F	ATCCAGTGCGTGTCGTG
miR-103a-3p-R	TGCTAGCAGCATTGTACAGG
miR-103a-3p mimics sense	AGCAGCAUUGUACAGGGCUAUGA
miR-103a-3p mimics antisense	AUAGCCCUGUACAAUGCUGCUUU
siRNA control sense	UUCUCCGAACGUGUCACGU
siRNA control antisense	ACGUGACACGUUCGGAGAA
miR-103a inhibitor	TCATAGCCCTGTACAATGCTGCT
Inhibitor control	CAGTACTTTTGTGTAGTACAA
ATF7-F	CCAACAGGCAAATGGGGTCT
ATF7-R	TAACTGGTGGGCCAGGGATA
siATF7-1 sense	CUCACCAAGUCUCCUCAAU
siATF7-1 antisense	AUUGAGGAGACUUGGUGAG
siATF7-2 sense	CUGAGCAUGCCGAUACAAU
siATF7-2 antisense	AUUGUAUCGGCAUGCUCAG
siRNA control sense	UUCUCCGAACGUGUCACGUTT
siRNA control antisense	ACGUGACACGUUCGGAGAATT
ATF7-WT-sense	CTATTGTGCCTTATTTATGCTGCAC
ATF7-WT-antisense	TCGAGTGCAGCATAAATAAGGCACAATAGAGCT
ATF7-MT-sense	CTATTGTGCCTTATTTAGTATCAC
ATF7-MT-antisense	TCGAGTGATACTAAATAAGGCACAATAGAGCT

transfected using jetPRIME (Polyplus Co., France), and the medium was replaced 4 h after transfection.

miRNA and RNA interference

The miR-103a-3p mimics and miRNA negative control (double-stranded non-human miRNAs predicted to not target the human genome/transcriptome) were synthesized at GenePharma Biotech (China). Antisense miR-103a-3p oligonucleotides were synthesized as inhibitors at Sangon Biotech (Shanghai, China). The inhibitor control was also synthesized at Sangon Biotech (China). The siRNA duplexes targeting human ATF7 were synthesized and purified at GenePharma Biotech (China). siRNA duplexes predicted to not target the human genome/transcriptome were used as siRNA negative controls. RNA oligonucleotides were transfected using jetPRIME (Polyplus Co., France), and the medium was replaced 4 h after transfection. miRNA or siRNA was used at a final concentration of 30 nmol/L. All oligonucleotide sequences are listed in Table 2.

Cell viability assay

Cells were washed with warm 1640, 3-(4,5-Dimethylthiazol-2-yl)-2,5-diphenyltetrazolium bromide (MTT)(Sigma, Germany) reagent was added, and the plates were incubated for 4 hours at 37℃. The supernatant was then discarded and replaced with dimethyl sulfoxide (DMSO). The absorbance of the converted dye was measured at 492 nm on a microplate reader (FLUOstar OPTIMA, BMG, Germany).

Colony formation assay

MKN-45/SGC-7901 cells were seeded in 6-well plates at 2000 cells per well, transfected 24 h later and incubated for ten days. Cells were washed with PBS and stained with 0.1% crystal violet for 30 min. Images were captured on a Bio-Rad Universal Hood Molecular Gel Imaging System (Bio-Rad, USA), and clones were counted using computer software (Bio-Rad Quantity One).

Cell-cycle analysis

For cell cycle analysis, the cells were detached via trypsinization, washed with PBS and fixed overnight in ice-cold ethanol at 4℃. Fixed cells were then washed with PBS and incubated in 0.5 ml of staining solution (0.1 mg/ml RNase A and 0.05 mg/ml propidium iodide) for 30 minutes at room temperature. Cell cycle distributions were detected by flow cytometry (FACSort; Becton Dickinson, USA) and analyzed using ModFit software.

Dual-luciferase reporter gene assay

The pmirGLO Dual-Luciferase Vector (Promega, USA) was used for the miRNA target detection assay. The putative miR-103a-3p-binding site in the ATF7 3' UTR was used to construct wild-type or mutant reporter duplexes (named WT for wild type and MT for mutant type; the sequences are listed in Table 2). All duplexes were chemically synthesized and cloned into the pmirGLO vector between the *Sac*I and *Xho*I sites according to the manufacturer's instructions (Dual-Luciferase Reporter Assay System, Promega, USA). Luciferase reporter gene assays were performed using HEK293 cells seeded in 96-well plates at 90% confluence. For the ATF7 3' UTR luciferase reporter assay, wild-type, mutant-type or empty pmirGLO vectors were cotransfected into HEK293 cells with 30 nmol/L miR-103a-3p using jetPRIME. Reporter gene assays were performed at 24 h post-transfection using the Dual-Luciferase Assay System (Promega, USA). The analysis was performed with three repeated experimental results.

Western blot analysis

For Western blotting, cells were lysed using RIPA buffer (Sigma-Aldrich, Germany). Lysates were then collected by centrifugation at 14, 000 × g for 20 min. Protein concentrations were determined using the BCA protein assay kit (Thermo Fisher, USA). Equal amounts of protein lysates were subjected to SDS-PAGE, transferred to methanol-activated PVDF membranes and blocked with 5% non-fat dry milk in Tris-buffered saline (pH 7.4) containing 0.1% Tween (TBST) for 2 h. A prestained ladder (Precision Plus Protein™ Dual Color Standards, Bio-Rad, USA) was used as a molecular size marker. The membranes were incubated overnight with primary antibodies (Abcam Biotechnology, UK) at 4℃. Anti-rabbit or anti-mouse (Santa Cruz Biotechnology, USA) secondary antibodies were then used for 1 h at room temperature. Protein expression was normalized to β-actin levels in each sample. All Western blotting analysis were repeated at least three times under similar conditions.

Bioinformatics analysis

The TCGA database with designed web tool (https://xenabrowser.net/) was used to investigate the relative expression of miR-103a-3p and ATF7 and determine the correlation between their expression levels in stomach cancer. For miRNA target prediction, two popular public databases, Targetscan (http://www.targetscan.org/vert_71/) and miRDB (http://mirdb.org/miRDB/), were used and crosschecked.

Statistical analysis

Data are expressed as the mean ± SEM from at least three separate experiments. The differences between groups were analyzed using Student's t test, except where noted. All tests were two-sided. Differences were considered statistically significant at $P < 0.05$. All statistical analyses were performed using SPSS 13.0 software (SPSS Inc, USA). The linear correlation coefficient (Pearson's r) was calculated to estimate the correlation between miR-103a-3p and ATF7 expression.

RESULTS

miR-103a-3p is frequently increased in both human gastric carcinoma tissue samples and in the TCGA database

To investigate the role of miR-103a-3p in GC, the expression of miR-103a-3p in 33 paired GC and adjacent nontumor stomach tissue samples was analyzed using qRT- PCR. Compared with their peritumor counterparts, a significant upregulation of miR-103a-3p was observed in 26 of 33 gastric cancer samples (Fig. 1A). Additionally, TCGA stomach cancer cohort analysis showed that miR-103a-3p was significantly upregulated based on either paired or unpaired data

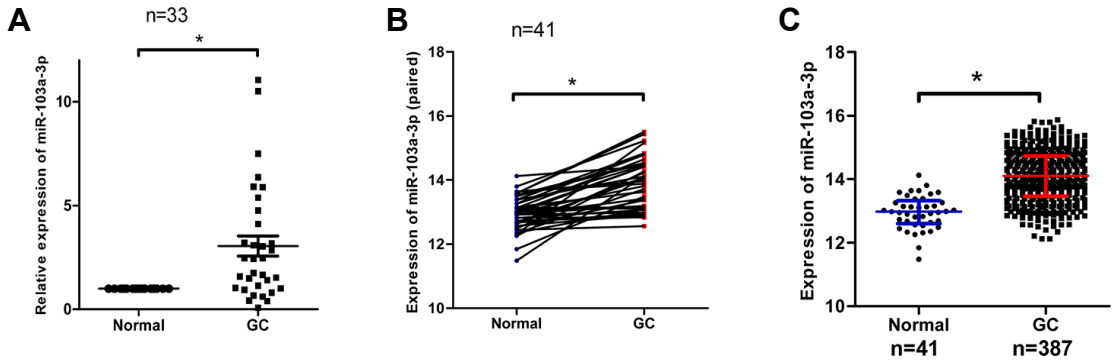

Fig. 1. Dysregulated miR-103a-3p expression in gastric cancer tissues. (A) qRT-PCR was performed to examine miR-103a-3p expression in 33 paired human gastric cancer tissues. Adjacent nontumor tissues were used as normal controls. (B) miR-103a-3p expression in the TCGA stomach cancer cohort (n = 41, paired). (C) miR-103a-3p expression in the TCGA stomach cancer cohort (unpaired) (*, $P < 0.05$; Student's t test).

(Figs. 1B and 2C), which matched the trend in the 33 paired gastric cancer tissues. In addition, we examined the correlation of miR-103a-3p levels with histological grade and tumor stage in the 33 paired GC tissue samples. miR-103a-3p expression was upregulated in 18 poorly differentiated tumor tissues (Table 3) or in 24 tumor stage III/IV samples (Table 4), indicating that miR-103a-3p may act as a tumor promoter in GC.

miR-103a-3p increases MKN-45/SGC-7901 cell growth, and miR-103a-3p overexpression promotes the S-G2/M transition *in vitro*

To explore the role of miR-103a-3p in GC, MKN-45/SGC-7901 cells were transfected with miR-103a-3p mimics or negative controls. qRT-PCR was performed to assess miR-103a-3p expression levels after transfection of miR-103a-3p mimics or the negative control. A greater than 70-fold increase of miR-103a-3p expression was observed in MKN-45/SGC-7901 cells transfected with 30 nmol/L miR-103a-3p relative to the cells transfected with 30 nmol/L miR-103a-3p negative control (Fig. 2A). MTT assays were used to investigate the role of miR-103a-3p in GC cell proliferation, showing that miR-103a-3p overexpression promoted the proliferation of MKN-45/SGC-7901 at 72 h after transfection (Fig. 2B). To further explore the tumor-contributor role of miR-103a-3p in GC cells, colony formation assays were used after a similar transient transfection. miR-103a-3p-transfected cells displayed a higher number and larger size of colonies compared with the negative control (Fig. 2C, quantification data for Fig. 2C is illustrated in Supplementary Fig. S3). Taken together, MTT and colony formation showed that miR-103a-3p promoted the proliferation of GC cells *in vitro*.

To further investigate the mechanisms through which miR-103a-3p promotes GC cell proliferation, Cell cycle assays were performed to detect the percentage of cells in the G1, S, and G2 phases with flow cytometry. MKN-45/SGC-7901 cells were transfected with miR-103a-3p or the negative control. Results showed that miR-103a-3p overexpression induced the accumulation of the G2/M-population (Fig. 2D, FACS data for Fig. 2D is illustrated in Supplementary Fig. S1), suggesting that miR-103a-3p promotes the S-G2/M transition.

In addition, miR-103a-3p inhibitor was used to validate the proliferative role of miR-103a-3p by eliminating endogenous miR-103a-3p in human GC cells. Reducing the endogenous expression of miR-103a-3p in MKN-45/SGC-7901 cells using miR-103a-3p inhibitor resulted in decreased cell viability and colony formation potential (Figs. 2E-2G; Quantification data for Fig. 2G is illustrated in Supplementary Fig. S4). Furthermore, cell-cycle analysis showed that inhibitor-transfected MKN-45/SGC-7901 cells were preferentially blocked in S-phase (Fig. 2H, FACS data for Fig. 2H is illustrated in Supplementary Fig. S2). These results suggested that the baseline expression of miR-103a-3p is sufficient to initiate proliferation during S-G2/M in GC cells, thereby stimulating further malignancy progression.

Table 3. The relationship between miR-103a-3p relative expression levels and tumor differential degree

Histologic grade	miR-103a-3p expression levels	
	>1	<1
well differentiated	0	0
moderate differentiated	8(80.00%)	2(20.00%)
Poor differentiated	18(78.26%)	5(21.74%)

Table 4. The relationship between miR-103a-3p relative expression levels and tumor stage

TNM stage	miR-103a-3p expression levels	
	>1	<1
I	2(66.67%)	1(33.33%)
II	0	2(100%)
III	22(84.62%)	4(15.38%)
IV	2(100%)	0

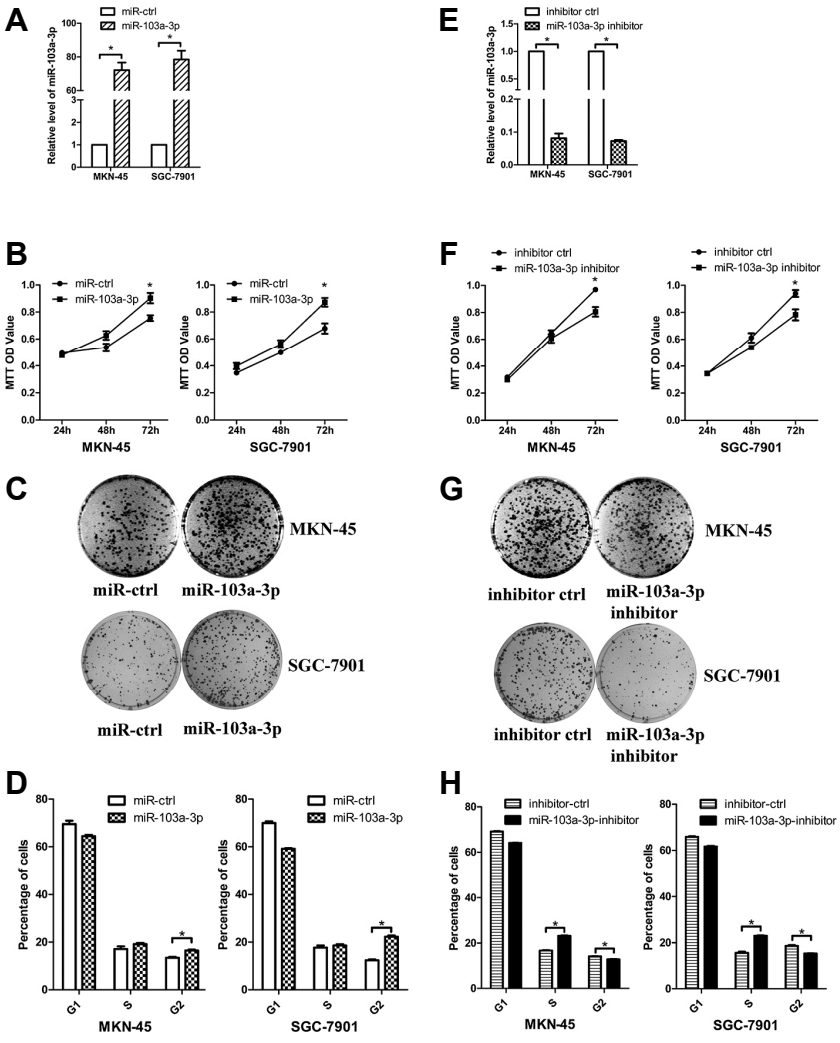

Fig. 2. miR-103a-3p facilitates MKN-45/SGC-7901 cell growth, and inhibiting miR-103a-3p induces S-G2/M arrest *in vitro*. (A) qRT-PCR analysis of miR-103a-3p in MKN-45/SGC-7901 cells transfected with miR-103a-3p mimics. Non-human miRNAs predicted to not target the human genome/transcriptome were used as negative controls. (B) The effects of miR-103a-3p on MKN-45/SGC-7901 cell proliferation were determined via MTT assays at 24, 48, and 72 h after transfection with miR-103a-3p mimics and negative controls. (C) Colony formation assays were performed to detect the effect of miR-103a-3p transfection in MKN-45/SGC-7901 cells. (D) Cell-cycle measurements in MKN-45/SGC-7901 cells 48 h after transfection. (E) qRT-PCR analysis of miR-103a-3p in MKN-45/SGC-7901 cells transfected with miR-103a-3p inhibitor. Non-human single-stranded oligos were used as negative controls. (F) MTT was used to assess the effects of miR-103a-3p inhibitor in MKN-45/SGC-7901 cells. (G) the growth of MKN-45/SGC-7901 cells was detected using colony formation assays. (H) The cell cycle was monitored in MKN-45/SGC-7901 cells transfected with miR-103a-3p inhibitor or negative controls (*, $P < 0.05$, Student's t test).

miR-103a-3p promotes gastric cancer cell proliferation by directly targeting ATF7

To reveal the mechanisms by which miR-103a-3p promotes the S-G2/M transition, we searched for miR-103a-3p target genes. Among many putative targets, ATF7 is of particular interest because of its transcription factor role in cellular functions. As we all know, transcription factors play important roles in cell proliferation, division and death. Deregulation of transcription factors is a pervasive theme across many forms of human cancer. Targeting transcription factors can be an effective way in treating cancer. As shown in Fig. 3A, a region complementary to miR-103a-3p seed region was identified in the 3' UTR of human ATF7. To validate whether ATF7 was a direct target of miR-103a-3p, a Dual-Luciferase Reporter System containing the wild-type or mutant 3' UTR of ATF7 was used. Cotransfecting miR-103a-3p with wild-type ATF7 vector induced low luciferase activity, whereas cotransfection with the mutant ATF7 vector had no effect (Fig. 3B), suggesting that miR-103a-3p directly and specifically bound the predicted binding site in the 3' UTR of ATF7. To identify whether miR-103a-3p expression affected endogenous ATF7 expression, miR-103a-3p, miR-103a-3p inhibitor or negative controls were transfected into MKN-45 cells. Decreased ATF7 protein levels were observed after transfection with miR-103a-3p, whereas cells transfected with miR-103a-3p inhibitor demonstrated an enhanced expression of ATF7 protein. No decrease was detected in ATF7 mRNA levels, indicating that miR103a-3p regulates ATF7 via translational silencing (Fig. 3C). To further investigate the relationship between ATF7 and miR-103a-3p, we also examined ATF7 expression levels in the TCGA stomach cancer cohort as well as the correlation between ATF7 and miR-103a-3p. We found that miR-103a-3p levels were inversely correlated with ATF7 expression (Fig. 3D). Taken together, the above data suggest that miR-103a-3p directly regulates ATF7 expression in GC cells.

Knocking down ATF7 mimics the effects of miR-103a-3p overexpression in gastric cancer cells

Two siRNAs were designed to silence ATF7 and were used to identify whether ATF7 is involved in the tumor-promoting effects of miR-103a-3p. ATF7 was specifically knocked down

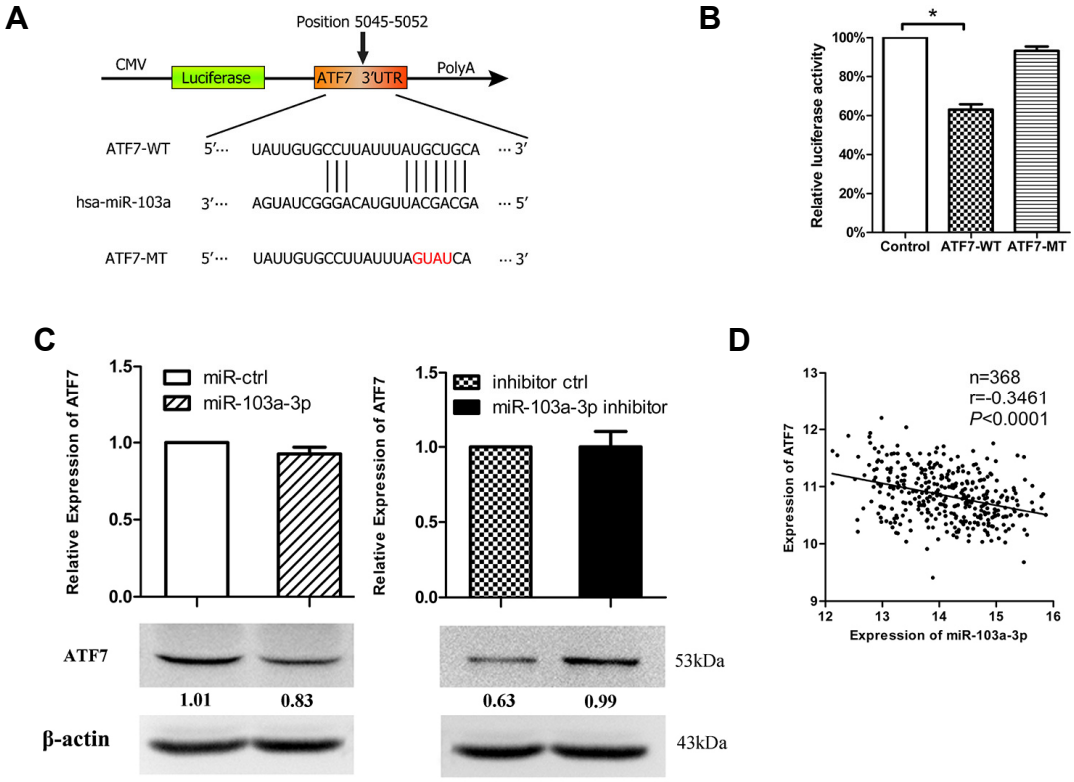

Fig. 3. miR-103a-3p promotes tumor proliferation by directly targeting ATF7 in gastric cancer. (A) Scheme of the potential binding sites of miR-103a-3p in the ATF7 3' UTR. (B) Luciferase assay in HEK293 cells. miR-103a-3p mimics were co-transfected with pmirGLO-ATF7-WT (wild type) 3' UTR or pmirGLO-ATF7-MT (mutant type) 3' UTR or control. Luciferase activity was measured at 24 h after transfection, and a significant decrease was detected in the pmirGLO-ATF7-WT group (*, $P < 0.05$). (C) ATF7 mRNA and protein expression levels were measured via qRT-PCR and Western blotting, respectively, in MKN-45 cells transfected with miR-103a-3p or miR-103a-3p inhibitor. The intensity for each band was quantified. The value under each lane indicates the relative expression level of the ATF7. (D) Inverse correlation between miR-103a-3p and ATF7 in the TCGA stomach cancer cohort (n = 368). Statistical analysis was performed using Pearson's correlation coefficient (r = -0.3461, $P < 0.05$).

by at least 90% at both the mRNA and protein level using siRNA in MKN-45/SGC-7901 cells (Figs. 4A and 4F). The results of MTT and colony formation assays revealed that in MKN-45 cells, ATF7 silencing stimulated cell proliferation, and cell-cycle analysis results showed that siATF7 increased the accumulation of cells at the G2/M phase (Figs. 4B-4D, quantification data for Fig. 4C is illustrated in Supplementary Fig. S5), consistent with the effects of miR-103a-3p overexpression. Similar proliferation effects after ATF7 silencing were also observed in SGC-7901 cells, which is consistent with miR-103a-3p overexpression as well (Figs. 4G-4I, quantification data for Fig. 4H is illustrated in Supplementary Fig. S5). In addition, Western blotting was used to analyze S-G2/M-related regulators after miR-103a-3p overexpression or ATF7 silencing in MKN-45 and SGC-7901 cells. As shown in Figs. 4E and 4J, both miR-103a-3p overexpression and ATF7 silencing promoted the expression of CDK2, an essential regulator of the S-G2/M transition. Furthermore, miR-103a-3p overexpression and ATF7 knockdown obviously decreased p27. Moreover, reducing the expression of miR-103a-3p using miR-103a-3p inhibitor showed adverse effects at the protein level. These results demonstrated that miR-103a-3p and its target gene ATF7 share similar cellular and molecular effects in both MKN-45 and SGC-7901 cells.

ATF7 overexpression eliminated the effects of miR-103a-3p

To further understand the role of miR-103a-3p in GC as a tumor promoter via ATF7, we constructed an ATF7 overexpression vector. MKN-45/SGC-7901 cells were transfected with the ATF7 overexpression vector, and an empty vector was used as a control. We observed a significant increase in both ATF7 protein and mRNA levels after transfection with the ATF7 overexpression vector (Fig. 5A). Upon cotransfection with miR-103a-3p and the ATF7 vector, ATF7 overexpression counterbalanced the tumor-stimulating effect of miR-103a-3p in GC cell proliferation (Fig. 5B). Cell-cycle assays were used to investigate the effect of ATF7 overexpression on cell-cycle progression in MKN-45/SGC-7901 cells. ATF7 overexpression blocked the S/G2 transition in MKN-45/SGC-7901 cells. Moreover, compared with the cotransfection of miR-103a-3p and ATF7-ctrl, cotransfection of miR-103a-3p and ATF7 also blocked the S/G2 transition in GC

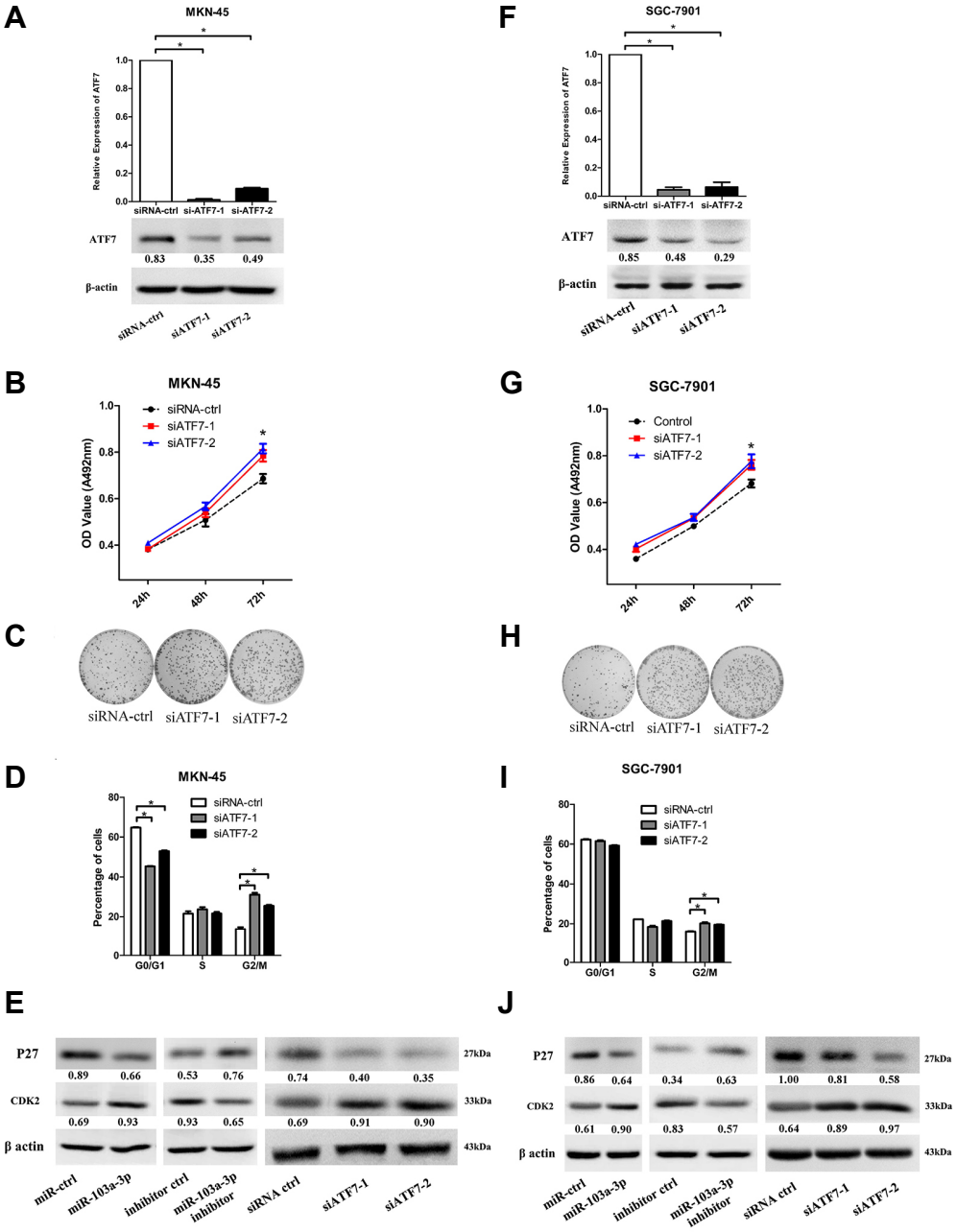

Fig. 4. miR-103a-3p promotes cell proliferation through AFT7. (A) qRT-PCR and Western blotting were performed to determine ATF7 expression levels after MKN-45 cells were transfected with two different short interfering RNAs against ATF7. The intensity for each band was quantified. The value under each lane indicates the relative expression level of ATF7. (B) MTT assays were performed to determine the growth of cells treated with siATF7s. (C) The growth of MKN-45 cells was detected based on colony formation after ATF7 knockdown. (D) The cell cycle was monitored in MKN45 cells at 48 h after ATF7 knockdown. (E) Protein expression analysis for ATF7-dependent cell-cycle regulation proteins in MKN-45 cells after transfected with miRNA control, miR-103a-3p, inhibitor control, miR-103a-3p inhibitor, siRNA negative control and siATF7s. The intensity for each band was quantified. The value under each lane indicates the relative expression level of the regulators. (F) Relative of ATF7 expression levels were detected using qRT-PCR and Western blotting after SGC-7901 cells were transfected with siATF7s. The intensity for each band was quantified. The value under each lane indicates the relative expression level of ATF7. (G) MTT assays were performed to determine the growth of SGC-7901 cells after siATF7 transfection. (H) The growth of SGC-7901 cells was detected based on colony formation after ATF7 knockdown. (I) The cell-cycle progression was monitored in SGC-7901 cells at 48 h after transfection with siATF7. (J) Western blotting of cell-cycle regulation proteins in SGC-7901 cells transfected with miRNA control, miR-103a-3p, inhibitor control, miR-103a-3p inhibitor, siRNA negative control and siATF7s. The intensity for each band was quantified. The value under each lane indicates the relative expression level of the regulators. (*, $P < 0.05$, Student's t test)

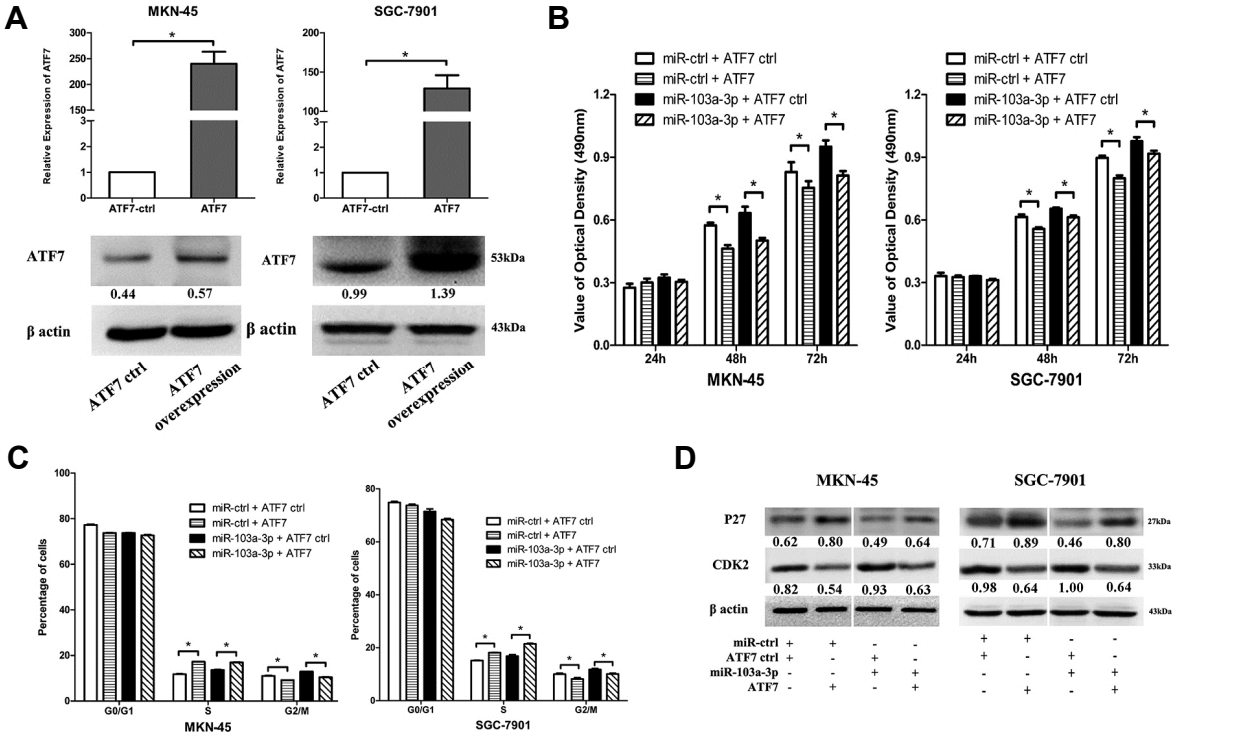

Fig. 5. ATF7 rescues the cellular phenotypes induced by miR-103a-3p in gastric cancer cells. (A) MKN-45/SGC-7901 cells were transfected with the ATF7 overexpression construct, with the empty vector used as a control. ATF7 expression levels were verified by qRT-PCR and Western blotting. The intensity for each band was quantified. The value under each lane indicates the relative expression level of ATF7. (B) MTT assays were performed to determine the growth of MKN-45/SGC-7901 cells cotransfected with ATF7 and miRNA control or control vector and miR-103a-3p. Cotransfection of ATF7 ctrl and miR-ctrl or ATF7 ctrl and miR-103a-3p were set as control group. (C) Flow cytometry was used to examine the cell cycle in MKN-45/SGC-7901 cells at 48 h after transfection. (D) Western blotting was used to assay the expression of cell-cycle regulators in both MKN-45 and SGC-7901 cells. The intensity for each band was quantified. The value under each lane indicates the relative expression level of the regulators. (*, $P < 0.05$, Student's t test).

cells (Fig. 5C). Furthermore, the expression of cell-cycle regulators was investigated using Western blotting after cotransfection. Compared with miR-ctrl and ATF7-ctrl cotransfection group, miR-ctrl and ATF7 cotransfection resulted in the downregulation of CDK2 in GC cells. Notably, compared with miR-103a-3p and ATF7-ctrl cotransfection, the expression of regulators was disrupted after cotransfection with miR-103a-3p and ATF7 (Fig. 5D).

Taken together, these results further suggest that miR-103a-3p has an oncogenic role in GC by directly targeting ATF7.

DISCUSSION

Over the past decades, studies have shown that the dysregulation of miRNAs can control cell proliferation in GC development and progression. miR-103a-3p, previously referred to as miR-103 or miR-103a, shows an increased expression in multiple cancers. In liver cancer, miR-103 potentially functions as an oncogene in hepatocellular carcinoma by inhibiting AKAP12 expression (Xia et al., 2016). In addition, miR-103 promotes cell proliferation and migration by targeting DICER and PTEN in colorectal cancer cells (Geng et al., 2014). These data suggest that miR-103a-3p is an oncogene. In GC, although there is debate over the expression level and function of miR-103a-3p in human GC (Liang et al., 2015), most research revealed that miR-103a-3p is upregulated in human GC studies (Shrestha et al., 2014). Additionally, mouse model study indicated that miR-103 was significantly upregulated in serum in both early and advanced-stage and considered promising biomarkers for early detection of gastric cancer (Rotkrua et al., 2013). Moreover, another study also demonstrated that high expression of miR-103 in advanced GC tissues may be a high risk factor associated with tumor penetration and poor long-term survival (Kim et al., 2013). Until now, few reports have investigated the function and underlying mechanisms of miR-103a-3p in GC.

The present research confirmed that miR-103a-3p was upregulated in 33 paired gastric cancer tissues, consistent with our findings in the TCGA stomach cancer cohort, suggesting that miR-103a-3p may be a tumor promoter in GC. To further explore the effect of miR-103a-3p *in vitro*, gain- and loss-of-function studies were performed. Overexpression of miR-103a-3p in GC cells promotes cell proliferation, clonogenicity, and enhances the S-to-G2/M transition, while inhibition of miR-103a-3p suppressed GC cell proliferation,

clonogenicity, and blocked the S-G2/M transition. This result verified the results previously reported in literatures, provided a more comprehensive understanding of the oncogenic role of miR-103a-3p during gastric cancer development.

To investigate the underlying mechanisms of miR-103a-3p in GC, bioinformatics and dual-luciferase reporter assays were used to identify the potential target through which miR-103a-3p regulates cell proliferation. An inverse correlation was observed between miR-103a-3p and ATF7 expression in the TCGA stomach cancer cohort, and dual-luciferase reporter assays confirmed that miR-103a-3p suppressed ATF7 expression by binding directly to its 3' UTR.

Studies on ATF7 are relatively scarce. ATF7 is primarily mentioned alongside ATF2, which is structurally very similar to ATF7, especially within the bZIP (basic region/leucine zipper) DNA-binding and dimerization domains (Vinson et al., 2002). ATF7 can form homodimers as well as heterodimers with c-jun or c-fos through its C-terminal leucine zipper region. Depending on the cellular context, the composition of the dimeric complexes determines the regulation of growth, survival or apoptosis (Vlahopoulos et al., 2008). In mice, B cell-specific deletion of ATF2 and ATF7 significantly accelerates the onset of *Em-Myc*-induced lymphoma. In addition, loss of ATF2/7 desensitizes *Em-Myc* lymphoma cells to spontaneous and stress-induced apoptosis (Walczynski et al., 2014). In colorectal cancer, ATF7 was negatively correlated with pathological stage and positively correlated with 5-year overall survival or 5-year progression-free survival (Guo et al., 2015b), suggesting that ATF7 may play a potential tumor suppressor role in colorectal cancer. To reveal the functions of ATF7 in GC, we overexpressed ATF7 and observed that ATF7-treated MKN-45/SGC-7901 cells showed a significant accumulation of ATF7 protein, consequently resulting in restricted cell proliferation, colony formation and the inhibition of the S-G2/M transition in both MKN-45 and SGC-7901 cells. Furthermore, ATF7 overexpression eliminated the effect of miR-103a-3p on GC cells, and ATF7 silencing improved the tumorigenic properties of GC cells, similar to that of miR-103a-3p overexpression. These results suggested that ATF7 may also act as a tumor suppressor in GC. Further gain- and loss-of-function experiments revealed that miR-103a-3p expression was positively correlated with the cell cycle-related protein CDK2 and that ATF7 expression was negatively correlated with CDK2 in GC cells. Moreover, P27 protein expression showed a positive trend compared with ATF7. These findings suggest that miR-103a-3p may contribute to cell-cycle progression by targeting ATF7 and regulating ATF7 related signaling pathways in GC, presenting the first evidence that increased ATF7 can indirectly downregulate CDK2 expression and upregulate P27 expression *in vitro*.

In summary, for the first time, we investigated the roles of miR-103a-3p and its target gene, ATF7, in controlling the cell cycle and their potential implication in pathological processes in GC cell lines. Moreover, we provided novel evidence that miR-103a-3p, as a tumor promoter, can enhance the growth of GC cells, suppress ATF7 expression and regulate related cell-cycle signaling pathways. These findings highlight the function of miR-103a-3p in GC cells, offering new insights into the regulatory network of the cell cycle, which may be a potential therapeutic strategy for the treatment of GC in the future.

Note: Supplementary information is available on the Molecules and Cells website (www.molcells.org).

ACKNOWLEDGMENTS

This study was funded by Opening Project of Key Laboratory of Shaanxi Province for Craniofacial Precision Medicine Research, College of Stomatology, Xi'an Jiaotong University (2016LHM-KFKT003).

REFERENCES

Arabpour, M., Mohammadparast, S., Maftouh, M., ShahidSales, S., Moieni, S., Akbarzade, H., Mirhafez, S.R., Parizadeh, S.M., Hassanian, S.M., and Avan, A. (2016). Circulating microRNAs as potential diagnostic biomarkers and therapeutic targets in gastric cancer: current status and future perspectives. Curr. Med. Chem. *23*, 4135-4150.

Bang, Y.-J., Van Cutsem, E., Feyereislova, A., Chung, H.C., Shen, L., Sawaki, A., Lordick, F., Ohtsu, A., Omuro, Y., and Satoh, T. (2010). Trastuzumab in combination with chemotherapy versus chemotherapy alone for treatment of HER2-positive advanced gastric or gastro-oesophageal junction cancer (ToGA): a phase 3, open-label, randomised controlled trial. The Lancet *376*, 687-697.

Bray, F., Ren, J.S., Masuyer, E., and Ferlay, J. (2013). Global estimates of cancer prevalence for 27 sites in the adult population in 2008. Int. J. Cancer *132*, 1133-1145.

Chen, H.Y., Lin, Y.M., Chung, H.C., Lang, Y.D., Lin, C.J., Huang, J., Wang, W.C., Lin, F.M., Chen, Z., Huang, H.D., et al. (2012). miR-103/107 promote metastasis of colorectal cancer by targeting the metastasis suppressors DAPK and KLF4. Cancer Res. *72*, 3631-3641.

Cho, W.J., Shin, J.M., Kim, J.S., Lee, M.R., Hong, K.S., Lee, J.H., Koo, K.H., Park, J.W., and Kim, K.S. (2009). miR-372 regulates cell cycle and apoptosis of ags human gastric cancer cell line through direct regulation of LATS2. Mol. Cells *28*, 521-527.

Garofalo, M., and Croce, C.M. (2011). microRNAs: Master regulators as potential therapeutics in cancer. Annu. Rev. Pharmacol. Toxicol. *51*, 25-43.

Geng, L., Sun, B., Gao, B., Wang, Z., Quan, C., Wei, F., and Fang, X.D. (2014). MicroRNA-103 promotes colorectal cancer by targeting tumor suppressor DICER and PTEN. Int. J. Mol. Sci. *15*, 8458-8472.

Gozdecka, M., and Breitwieser, W. (2012). The roles of ATF2 (activating transcription factor 2). in tumorigenesis. Biochem. Soc. Trans. *40*, 230-234.

Guo, C., Song, W.Q., Sun, P., Jin, L., and Dai, H.Y. (2015a). LncRNA-GAS5 induces PTEN expression through inhibiting miR-103 in endometrial cancer cells. J. Biomed. Sci. *22*, 100.

Guo, H.Q., Ye, S., Huang, G.L., Liu, L., Liu, O.F., and Yang, S.J. (2015b). Expression of activating transcription factor 7 is correlated with prognosis of colorectal cancer. J. Cancer Res. Therapeut. *11*, 319-323.

Hong, Z., Feng, Z., Sai, Z., and Tao, S. (2014). PER3, a novel target of miR-103, plays a suppressive role in colorectal cancer *in vitro*. BMB Rep. *47*, 500-505.

Kim, B.H., Hong, S.W., Kim, A., Choi, S.H., and Yoon, S.O. (2013). Prognostic implications for high expression of oncogenic microRNAs in advanced gastric carcinoma. J. Surg. Oncol. *107*, 505-510.

Koizumi, W., Narahara, H., Hara, T., Takagane, A., Akiya, T., Takagi, M., Miyashita, K., Nishizaki, T., Kobayashi, O., and Takiyama, W.

(2008). S-1 plus cisplatin versus S-1 alone for first-line treatment of advanced gastric cancer (SPIRITS trial).: a phase III trial. Lancet Oncol. *9*, 215-221.

Koizumi, W., Kim, Y.H., Fujii, M., Kim, H.K., Imamura, H., Lee, K.H., Hara, T., Chung, H.C., Satoh, T., and Cho, J.Y. (2014). Addition of docetaxel to S-1 without platinum prolongs survival of patients with advanced gastric cancer: a randomized study (START). J. Cancer Res. Clin. Oncol. *140*, 319-328.

Liang, J., Liu, X., Xue, H., Qiu, B., Wei, B., and Sun, K. (2015). MicroRNA-103a inhibits gastric cancer cell proliferation, migration and invasion by targeting c-Myb. Cell Proliferation *48*, 78-85.

Lin, Y., Nie, Y., Zhao, J., Chen, X., Ye, M., Li, Y., Du, Y., Cao, J., Shen, B., and Li, Y. (2012). Genetic polymorphism at miR-181a binding site contributes to gastric cancer susceptibility. Carcinogenesis *33*, 2377-2283.

Livak, K.J., and Schmittgen, T.D. (2001). Analysis of relative gene expression data using real-time quantitative PCR and the $2^{-\Delta\Delta CT}$ method. Methods *25*, 402-408.

Nonaka, R., Miyake, Y., Hata, T., Kagawa, Y., Kato, T., Osawa, H., Nishimura, J., Ikenaga, M., Murata, K., Uemura, M., et al. (2015). Circulating miR-103 and miR-720 as novel serum biomarkers for patients with colorectal cancer. Int. J. Oncol. *47*, 1097-1102.

Rotkrua, P., Shimada, S., Mogushi, K., Akiyama, Y., Tanaka, H., and Yuasa, Y. (2013). Circulating microRNAs as biomarkers for early detection of diffuse-type gastric cancer using a mouse model. Br. J. Cancer *108*, 932-940.

Shen, L., Shan, Y.-S., Hu, H.-M., Price, T.J., Sirohi, B., Yeh, K.-H., Yang, Y.-H., Sano, T., Yang, H.-K., and Zhang, X. (2013). Management of gastric cancer in Asia: resource-stratified guidelines. Lancet Oncol. *14*, e535-e547.

Shin, V.Y., Jin, H., Ng, E.K., Cheng, A.S., Chong, W.W., Wong, C.Y., Leung, W.K., Sung, J.J., and Chu, K.-M. (2011). NF-κB targets miR-16 and miR-21 in gastric cancer: involvement of prostaglandin E receptors. Carcinogenesis *32*, 240-245.

Shivers, R.P., Pagano, D.J., Kooistra, T., Richardson, C.E., Reddy, K.C., Whitney, J.K., Kamanzi, O., Matsumoto, K., Hisamoto, N., and Kim, D.H. (2010). Phosphorylation of the conserved transcription factor ATF-7 by PMK-1 p38 MAPK regulates innate immunity in Caenorhabditis elegans. PLoS Genet. *6*, e1000892.

Shrestha, S., Hsu, S.D., Huang, W.Y., Huang, H.Y., Chen, W., Weng, S.L., and Huang, H.D. (2014). A systematic review of microRNA expression profiling studies in human gastric cancer. Cancer Med. *3*, 878-888.

Strong, V.E., Wu, A.w., Selby, L.V., Gonen, M., Hsu, M., Song, K.Y., Park, C.H., Coit, D.G., Ji, J.f., and Brennan, M.F. (2015). Differences in gastric cancer survival between the US and China. J. Surg. Oncol. *112*, 31-37.

Tanabe, K., Suzuki, T., Tokumoto, N., Yamamoto, H., Yoshida, K., and Ohdan, H. (2010). Combination therapy with docetaxel and S-1 as a first-line treatment in patients with advanced or recurrent gastric cancer: a retrospective analysis. World J. Surg. Oncol. *8*, 40.

Vinson, C., Myakishev, M., Acharya, A., Mir, A.A., Moll, J.R., and Bonovich, M. (2002). Classification of human B-ZIP proteins based on dimerization properties. Mol. Cell Biol. *22*, 6321-6335.

Vlahopoulos, S.A., Logotheti, S., Mikas, D., Giarika, A., Gorgoulis, V., and Zoumpourlis, V. (2008). The role of ATF-2 in oncogenesis. Bioessays *30*, 314-327.

Walczynski, J., Lyons, S., Jones, N., and Breitwieser, W. (2014). Sensitisation of c-MYC-induced B-lymphoma cells to apoptosis by ATF2. Oncogene *33*, 1027-1036.

Wang, X., Wu, X., Yan, L., and Shao, J. (2012). Serum miR-103 as a potential diagnostic biomarker for breast cancer. Nan fang yi ke da xue xue bao = J. Southern Med. Univ. *32*, 631-634.

Wu, Q., Yang, Z., Wang, F., Hu, S., Yang, L., Shi, Y., and Fan, D. (2013). MiR-19b/20a/92a regulates the self-renewal and proliferation of gastric cancer stem cells. J. Cell Sci. *126*, 4220-4229.

Xia, W., Ni, J., Zhuang, J., Qian, L., Wang, P., and Wang, J. (2016). MiR-103 regulates hepatocellular carcinoma growth by targeting AKAP12. Int. Biochem. Cell Biol. *71*, 1-11.

Zheng, Y.B., Xiao, K., Xiao, G.C., Tong, S.L., Ding, Y., Wang, Q.S., Li, S.B., and Hao, Z.N. (2016). MicroRNA-103 promotes tumor growth and metastasis in colorectal cancer by directly targeting LATS2. Oncol. Lett. *12*, 2194-2200.